Catalysis Today 445 (2025) 115053

Contents lists available at ScienceDirect

Catalysis Today

journal homepage: www.elsevier.com/locate/cattod

Combining photocatalytic and adsorption units for the partial oxidation of tyrosol to hydroxytyrosol

Hiba Khlifi [a], Filippo Parisi [b], Luciana Sciascia [c], Leonardo Palmisano [d,*], Francesco Parrino [e,*]

[a] Laboratoire de Recherche Catalyse et Matériaux Pour l'Environnement et les Procédés. URCMEP (UR11ES85), Faculté des Sciences de Gabès/Université de Gabès, Campus Universitaire Cité Erriadh, Gabès 6072, Tunisia
[b] Department of Mathematics, Informatics and Geosciences, University of Trieste, Via E. Weiss 2, Trieste 34128, Italy
[c] Department of Earth and Marine Sciences, University of Palermo, Via Archirafi, 22, Palermo 90123, Italy
[d] Department of Engineering, University of Palermo, Viale delle Scienze, Ed. 16, Palermo 90128, Italy
[e] Department of Industrial Engineering, University of Trento, Via Sommarive 9, Trento 38123, Italy

ARTICLE INFO

Keywords:
Hydroxytyrosol
TiO_2
Selective adsorption
Flow chemistry
Photocatalysis

ABSTRACT

Photocatalytic partial oxidation of tyrosol (Tyr) to hydroxytyrosol (Htyr) which is a valuable antioxidant compound, was carried out in a fully recirculated flow photoreactor under UVA light irradiation by using as photocatalyst bare or fluorinated TiO_2 immobilized on glass beads. The maximum selectivity towards Htyr obtained under optimized conditions in the presence of fluorinated TiO_2 at pH 8.7 was approximately 12 %. Reducing the residence time did not result in any further improvement of reaction selectivity due to the fast overoxidation of Htyr.

The photocatalytic reactor was then coupled with an adsorption unit containing a home-made adsorbent exposing amine-stabilized boronate moieties, which showed negligible interaction with Tyr but was capable of selectively binding Htyr on its surface. This allowed for the complete recirculation of the reactant Tyr to the reactor, while the desired product Htyr could be selectively removed from the reaction medium, significantly limiting its parasitic overreaction. Consequently, performing the reaction in the coupled system doubled the selectivity towards Htyr for all configurations, providing a maximum selectivity of 25 % under optimized conditions, which is twice the highest value ever reported for this photocatalytic reaction.

Finally, the kinetic experimental data were modeled using the Copasi software package to elucidate the reaction pathway and estimate the apparent kinetic parameters of the photocatalytic process, both alone and in combination with the adsorption unit. The simulated results showed excellent agreement with the experimental data.

1. Introduction

Hydroxytyrosol (Htyr, 2-(3,4-dihydroxyphenyl)ethanol) is one of the most powerful antioxidant in nature, mostly found in leaves and fruits of olive trees [1]. Htyr exerts important bioactive functions, such as providing protection against oxidative stress in cells, acting as good transporter of substances through the human body due to its amphiphilic nature, and exhibiting anti-inflammatory, anticarcinogenic, antimicrobial, immunomodulatory, cardioprotective and neuroprotective activity [2]. These outstanding properties, along with the growing demand for natural ingredients in pharmaceutical, food and beverages, and cosmetic (especially for antiage products) industries, justify the high economic value of this compound. The Htyr market accounts for 2.3 billion dollars in 2023 and is forecasted, by the end of 2033, to rake in revenue for 4.6 billion dollars [3].

Nowadays, the main industrial method for Htyr production is its extraction from olive vegetation water [4,5], a process which generally affords mixtures of Htyr and tyrosol (Tyr, 2-(3-hydroxyphenyl)ethanol), which has much lower economic value. The increasing worldwide demand for Htyr combined with the limitations of current extraction processes (large use of solvents such as hexane and ethyl acetate, multi-step, low yield, and time demanding steps), recently boosted the research towards novel and more efficient Htyr production methods. Htyr can be synthesized generally starting from the corresponding carboxylic acid [6], or from other molecules such as catechol [7] and homovanillyl alcohol [8], using various types of protocols many of

* Corresponding authors.
E-mail addresses: leonardo.palmisano@unipa.it (L. Palmisano), francesco.parrino@unitn.it (F. Parrino).

https://doi.org/10.1016/j.cattod.2024.115053
Received 6 August 2024; Received in revised form 5 September 2024; Accepted 12 September 2024
Available online 13 September 2024

which are summarized in a recent review [9]. The use of Tyr as the reactant is promising [10], by considering that both compounds are present in olive extracts, which can be therefore enriched in the more valuable Htyr component (Fig. 1).

Several synthetic protocols starting from Tyr have been proposed (see Bouguerra Neji et al. [11] and references therein), but green and sustainable processes are required given the use of Htyr in food and health care products.

Traditionally used as a tool for environmental remediation, heterogeneous photocatalysis has been recently proposed as a promising green technology for selective chemical synthesis under mild conditions [12,13]. In particular, following the absorption of photons, in a photocatalyst such as TiO_2, charges are formed that induce redox reactions. In an oxygenated aqueous medium, mainly oxygen species are obtained that can potentially react (Reacting Oxygen Species, ROS) [14,15].

Among these, OH radicals can be produced efficiently, suggesting that the hydroxylation of Tyr to Htyr should occur without major difficulties under photocatalytic conditions. Unfortunately, the selectivity towards Htyr in the presence of bare powdered TiO_2 is extremely low because, once generated, this catecholic compound undergoes fast oxidation and does not significantly accumulate in the reacting medium, especially in batch systems. This problem has been preliminarily mitigated by fluorinating the surface of TiO_2 in order to reduce the affinity of Htyr for the surface of the photocatalyst [16]. As a result, the selectivity towards Htyr could be increased ten times with respect to the reaction performed in the presence of bare TiO_2. However, under the best operating conditions, the maximum selectivity value obtained was only 10 %.

The present work was aimed at further improving the selectivity of the reaction by carrying it out in a fully recirculated flow reactor and introducing an adsorption unit for the selective separation of Htyr during the process.

Continuous flow reactors are highly desirable for industrial applications, because they provide several advantages over batch systems, such as the potential for automation, easy scale-up of the system, low construction and operating costs, enhancement in quality control and real time monitoring [17,18]. Moreover, in the case of photocatalytic partial oxidation reactions, this reactor configuration may allow for optimization of selectivity, by opportunely tuning the residence time [19,20].

Another way to increase the selectivity of a photocatalytic partial oxidation is to selectively remove the target compound from the reacting medium while being produced, thereby preventing its overoxidation. This approach has been exploited for the recovery of high value added compounds such as aldehydes, by coupling a photocatalytic reactor with a membrane separation unit [21,22]. For instance, in the case of the photocatalytic synthesis of vanillin, pervaporation [22] or dialysis [23] membrane separation allowed to increase the selectivity towards the product [24]. In the present work this task has been faced by using an adsorbent material that exhibits negligible affinity for phenolic compounds such as Tyr, but is capable of removing from the reacting medium catecholic compounds such as Htyr. In this way, similarly to the membrane approach described above, Htyr could be selectively separated from the reacting medium, thus avoiding its overoxidation while the reactant could be recycled to the photocatalytic reactor. The adsorbent used in this investigation has been synthesized in our laboratory by modifying the surface of a commercial TiO_2 sample with amino and boronic moieties. The synthetic procedure, the characterization and the mechanism of selective binding of the catecholic moiety with the boronate groups have been thoroughly described in our previous paper [25]. More recently, an in-depth analysis of the adsorption mechanism of catechol and phenol onto this material has been also reported [26]. By taking advantage of the extensive knowledge acquired on this adsorbent material, we hereby report on its effects on the selectivity of the photocatalytic partial oxidation of Tyr towards Htyr. Finally, Tyr conversion kinetics was investigated and modelled to elucidate the reaction pathway and to estimate the effects of different experimental conditions on the apparent kinetic rate constants.

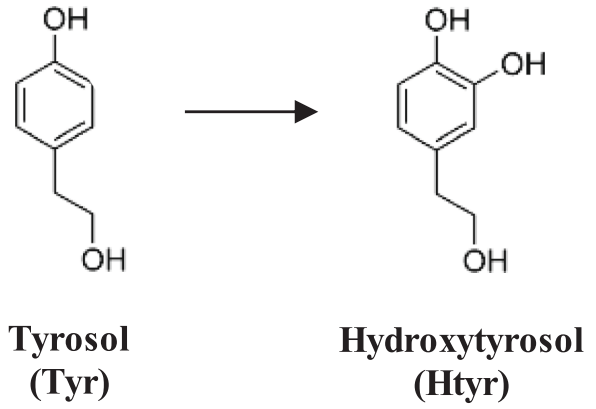

Fig. 1. Hydroxylation of tyrosol (Tyr) to hydroxytyrosol (Htyr).

2. Material and methods

2.1. Experimental set-up and modeling

Fig. 2 shows the experimental set-up.

The experimental set-up consisted of a cylindrical borosilicate photoreactor, an adsorbent bed, and a tank. The materials used to build the set-up (borosilicate glass for the reactor, Pyrex glass for adsorbent vessel and tank, and Chem-Durance-Bio® for tubing) did not adsorb dissolved organics and were inert. The photocatalytic reactor (internal diameter 20 mm, length 300 mm) was packed with 490 glass beads (diameter 4 mm) onto which TiO_2 P25 (Evonik, ca. 80 % anatase and 20 % rutile, specific surface area ca. 50 m^2/g) was deposited as described in Section 2.2. The reactor was placed within a wooden box to avoid irradiation of the other parts of the set-up, and was externally irradiated in hexagonal geometry by 6 actinic lamps (Philips, 14 W each, emission spectrum centred at 365 nm), each of them 75 mm distant from the axis of the reactor. The radiation intensity impinging on the reactor was measured by a radiometer Delta Ohm DO9721 with an UVA probe. When only one

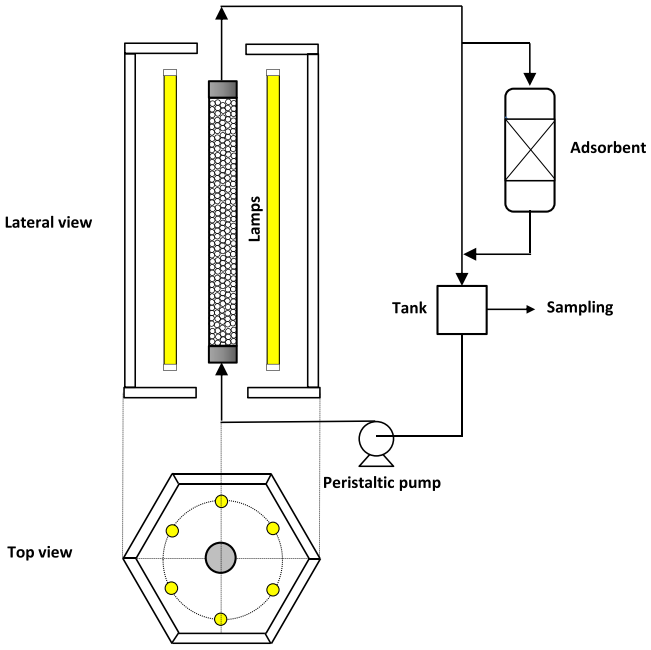

Fig. 2. Experimental set-up.

lamp was on, the photon flux incident on the reactor wall nearest to the lamp was 7.2 W/m^2. The adsorbent bed was placed in a cylindrical cartridge containing 12 mg of a surface modified TiO_2 P25 sample, prepared as described in Section 2.3. During the photocatalytic runs, the liquid solution exiting the reactor passed through the adsorbent bed and was continuously recirculated back by a peristaltic pump, after passing through a perfectly mixed tank (a 250 mL two necks round bottom flask, partially filled), whose task was to aerate the solution. Prior to irradiation, the solution was recirculated, by excluding the adsorbent bed, for 60 min in the dark in order to attain adsorbtion/desorption equilibrium of Tyr onto the photocatalytic bed. The flow rate ranged between 30 and 134 mL/min and the operating temperature was about 25 °C, maintained by means of a cooling air flow during irradiation. The circulating aqueous solution had an initial concentration of 0.5 mM Tyr and the natural pH was 5.5. Selected tests were performed by adjusting the pH of the solution at 8.7, *i.e.* the pk_a of the boronic moiety, by adding an opportune amount of NaOH. Samples of the flowing solution (1 mL each) were withdrawn from the tank at fixed times, filtered with a 0.2 μm Whatman PTFE microfilter, and analyzed by a Shimadzu HPLC Prominence equipped with a Shimpack GWS C18, 5 μm, 150 × 4.6 mm column and a diode array UV–vis detector. The eluent consisted of a solution containing 90 % v/v of a 1 % v/v CH_3COOH aqueous solution and 10 % v/v acetonitrile. The HPLC chromatograms were obtained at 280 nm, the flow rate was 1 mL/min, and the injection volume was 20 μL. The amount of Tyr and Htyr adsorbed onto the adsorbent bed was measured after each run, by washing the adsorbent bed 5 times with fixed volumes of an aqueous HCl solution (pH = 2.3), which was analysed as described above by means of HPLC. The photocatalytic bed was regenerated after each run by recirculating bi-distilled water under UV irradiation during 120 min. The trend of the selectivity during time in the coupled system was obtained by performing the same run three times, and each one stopped at 8, 15 and 30 min, respectively. The photocatalytic activity of the bed was regularly tested by performing the degradation of formic acid and by verifying that the rate of reaction did not significantly change. Formic acid was chosen as it undergoes direct mineralization without formation of other intermediates. Kinetic data from photocatalytic runs with or without the adsorption unit were modeled by using the Copasi Software [27].

2.2. Preparation of the photocatalytic bed

The immobilization of TiO_2 P25 onto glass beads was carried out by slightly modifying a procedure elsewhere reported [28], and here briefly described. 6 g of titanium tetraisopropoxide (TTIP, Sigma-Aldrich, 97 %) was mixed with diethanolamine (Riedel de Haën, 99 %) in molar ratio 1: 4 and the mixture was subsequently dissolved in 27 g of 2-propanol (Sigma-Aldrich, 99 %) and left stirring 2 h at room temperature. Demineralized water in molar ratio H_2O/TTIP = 2 was added slowly to the mixture, to induce hydrolysis of the alkoxide. 40 g/L of TiO_2 P25 was added to the solution and the suspension was vigorously stirred for 12 h, after being sonicated for 15 min. The obtained suspension was then used for the sol-gel deposition of six TiO_2 layers. Prior to deposition, 100 g of the glass beads were chemically etched by dipping them for 24 h in an 8 % v/v aqueous solution of HF (Sigma-Aldrich, 48 %) to make rougher the surface of the beads and allow better adhesion of the film. The beads were then rinsed with distilled water and dried at 80°C overnight.

For each TiO_2 layer deposition, the beads were dipped into the TiO_2 suspension for 30 min. Afterward, they were allowed to drain the solution in excess for 2 min, placed in a Pyrex tube at 150 °C for 2.5 h in the presence of a slow air flow, and finally calcined at 550 °C for 3.5 h. This procedure was repeated six times to increase the thickness of the film and to improve its mechanical stability. It was observed that further layer deposition did not increase the rate of photocatalytic mineralization of formic acid (tested as described before), so no additional layers were added.

Selected runs were performed in the presence of fluorinated TiO_2. Fluorination was performed after immobilization on glass beads, in the experimental set-up described above. A 4 % v/v aqueous solution of KF (Sigma-Aldrich, p.a.), with a pH adjusted to 3.2 using HNO_3, was flowed through the packed reactor for 8 hours in the dark. These experimental conditions maximized the amount of fluorine adsorbed at the surface of TiO_2, according to the relevant literature [29]. Thereafter, the photocatalytic bed was rinsed with distilled water and dried at 70°C overnight.

The thickness of the film and the atomic distribution was measured by means of a SEM-EDAX mapping (FE-SEM, Supra 40/40VP equipped with an EDAX probe, Zeiss, Oberkochen, Germany), operating at a voltage of 20 kV on a specimen prepared by embedding few beads in a polystyrene resin which was then smoothed in order to evidence the beads cross section. Prior to analysis, a 6 nm thin layer of Pt/Pd was deposited on the sample under Ar atmosphere. The cross-section micrograph and the EDAX mapping of the supported TiO_2 layer covering a glass bead are reported in Fig. 3a and b-c, respectively.

The surface of the glass beads exhibited significant roughness and porosity due to the HF etching. The TiO_2 layer was observed both at the surface and within the cracks. The film appeared to be composed of spherical microstructures, likely resulting from TiO_2 P25 aggregates embedded within a continuous network of TiO_2 formed upon hydrolysis and calcination of the TTIP precursor. The thickness of the film was ca. 40 μm. The total amount of catalyst present in the fixed bed was 0.12 g. This value was calculated by measuring the weight of the covered beads before and after the deposition. The BET specific surface area of the TiO_2 layer was about 60 m^2/g as measured by using the single-point BET method using a Micromeritics Flow Sorb 2300 apparatus.

2.3. Preparation of the adsorbent

The adsorbent bed consisted of TiO_2 P25 (Evonik) modified with amino and boronic groups, prepared as elsewhere reported [25]. A scheme detailing the modification steps (Figure S1), along with additional figures (Figures S2-S3) and a table (Table S1) summarizing the main physicochemical properties of the material as described in the literature, has been provided in the Supplementary Information Section for the reader's convenience. This modification minimizes interactions with phenolic compounds such as Tyr, while simultaneously allowing selective adsorption of catecholic compounds such as Htyr, as demonstrated in previous reports [26].

Briefly, the surface of TiO_2 was initially silanized with 3-aminopropyltrimethoxysilane (APTMS, Sigma-Aldrich, 97 %). In particular, 1 g of TiO_2 was dispersed in 50 mL of anhydrous toluene (Alfa Aesar, 99.8 %), sonicated for 15 minutes, and stirred for 1 h. Subsequently, 2.4 mL of APTMS were added drop-wise to the suspension, which was kept for 24 h at 85°C under vigorous agitation. Thereafter, the solid was separated by centrifugation (5000 rpm for 15 minutes), washed five times using anhydrous toluene, and finally dried under vacuum at 70 °C. 1 g of the resulting powder was further modified by reaction with an excess of 4-carboxyphenylboronic acid (CPBA, Sigma-Aldrich, p.a.) in 30 mL of anhydrous methanol (Sigma-Aldrich, 99.8 %) for 24 h under dark conditions. The obtained powder was separated by centrifugation, washed five times with methanol, and dried overnight at 70°C.

3. Results and discussion

3.1. Optimization of the photocatalytic flow reaction

Preliminary experiments were carried out to evaluate the influence of some operating parameters on the photocatalytic flow reaction performance in the presence of the bare TiO_2 packed bed and by-passing the adsorption unit. The influence of the flow rate on the Tyr partial oxidation and on the selectivity towards Htyr is reported in Fig. 4a and b, respectively, by taking constant the reaction volume (120 mL) and at

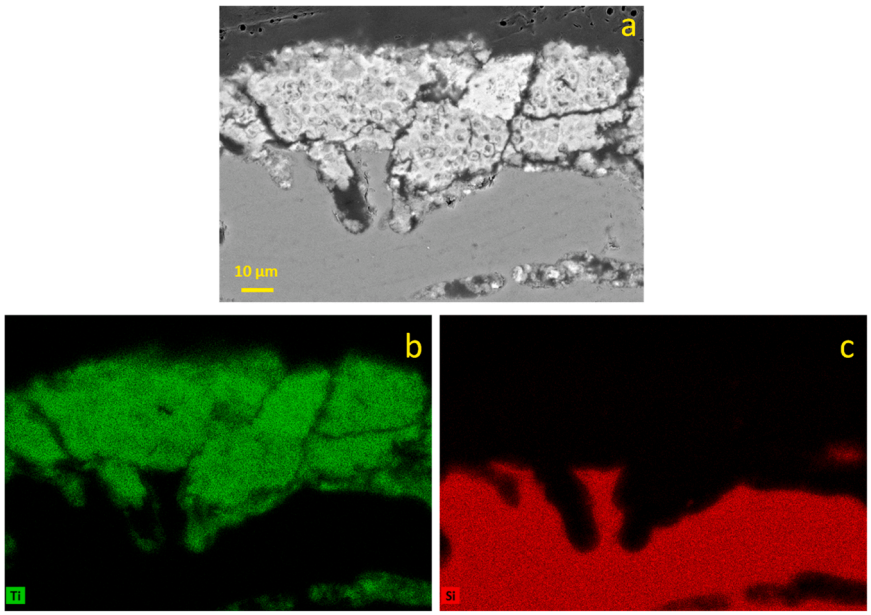

Fig. 3. SEM-EDAX analysis of the glass beads supporting the TiO_2 film used in the fixed bed reactor. a: cross section micrograph, b: mapping of titanium atoms (green points), c: mapping of silicon atoms (red points).

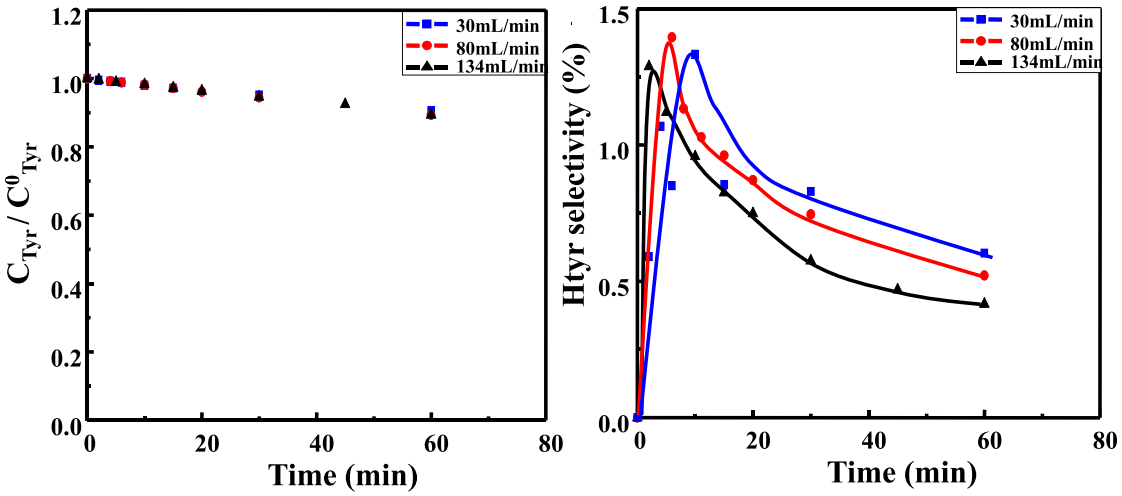

Fig. 4. Effect of the flow rate on the normalized concentration of Tyr (a) and selectivity towards Htyr (b). Reaction volume 120 mL, initial Tyr concentration C^0_{Tyr} = 0.5 mM, pH = 5.5.

natural pH 5.5.

Changing the flow rate from 30 to 134 mL/min did not affect the conversion of Tyr as expected, nor did it alter the maximum selectivity value obtained towards Htyr, which was ca. 1.3 % for all of the runs. The only observable effect was related to the time at which the maximum value of selectivity could be obtained, which was shifted towards shorter reaction times with increasing the flow rate from 30 to 134 mL/min, i.e. with reducing the residence time from 4 to 0.89 min. This reduction was not sufficient to increase the selectivity towards Htyr, indicating that the reaction's selectivity might likely benefit from being performed in more suitable microreactors.

A more pronounced effect on the selectivity of the reaction was observed by increasing the total volume, keeping constant the other parameters. Results are shown in Fig. 5.

No effects on the reaction rate can be observed, as the slope of the degradation curves in Fig. 5a doubles by halving the reaction volume from 240 (residence time 1.8 min) to 120 mL (residence time 0.89 min). On the other hand, the highest achievable selectivity is significantly reduced. Notably, in agreement with the results of Fig. 4, the maximum value of selectivity is shifted towards longer reaction times with increasing residence time.

According to these results, subsequent experiments have been carried out at a flow rate of 30 mL/min and with a total volume of 120 mL.

Previous studies on Tyr partial oxidation in batch systems showed that surface fluorination did not significantly alter the reaction conversion, while being beneficial in terms of selectivity towards Htyr. In particular, selectivity values up to 10 times higher than those obtained with the bare sample could be obtained in the presence of fluorinated P25 Evonik TiO_2 [16]. It has been proposed that the increased production of hydroxyl radicals and the lower hydrophilicity of the surface of the fluorinated sample favour hydroxylation of Tyr and desorption of Htyr, respectively, thus hindering the overoxidation of Htyr and increasing the selectivity.

The influence of surface fluorination on conversion and selectivity of the partial oxidation of Tyr to Htyr has been also investigated in the present flow system. Two different pH values, i.e. 5.5 and 8.7 were

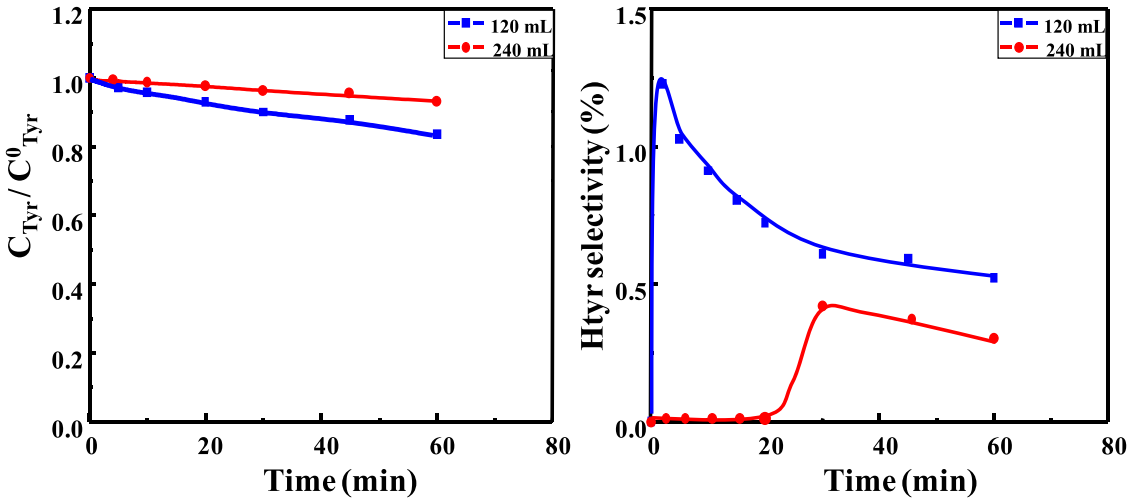

Fig. 5. Effect of Tyr initial volume on the normalized concentration of Tyr (a) and Htyr selectivity (b). Flow rate 134 mL/min, initial Tyr concentration C^0_{Tyr} = 0.5 mM, pH = 5.5.

selected. Results are shown in Fig. 6.

In agreement with previous results, fluorination did not significantly alter the reaction conversion. Instead, the selectivity values increased by two and ten times in the presence of fluorinated TiO_2, at pH = 5.5 and 8.7, respectively. The reader is referred to Khlifi et al. [16] for a detailed discussion on mechanistic aspects related to the influence of surface fluorination on conversion and selectivity of this reaction.

On the other hand, the effect of pH deserves here more attention. The increase in selectivity towards Htyr in the presence of fluorinated TiO_2 was more significant at alkaline pH.

This can be explained by considering the reduced interaction of hydroxytyrosol with the surface at alkaline pH. In fact, while the zero point charge of bare TiO_2 is reported to be ca. 6.3, that of fluorinated TiO_2 is ca. 4 [30]. Therefore, at each pH value above 4, the surface of fluorinated sample is always more negatively charged compared to the bare sample. By considering that both the OH groups of hydroxytyrosol are protonated under the present conditions, (pK_{a1} and pK_{a2} are 9.45 and 13, respectively) [31] chemisorption of Htyr through the catecholic moiety is hindered at both the pH values, and this effect is more pronounced at alkaline pH. The reduced interaction between Htyr and the surface of the photocatalyst under these conditions hinders its over-oxidation and results in the observed selectivity enhancement.

By concluding this preliminary part, fluorination is confirmed being a viable strategy to enhance the selectivity towards Htyr even in flow photocatalytic systems. However, reducing the residence time in the considered range did not result in improved selectivity, probably because of the fast kinetics of photocatalytic degradation of Htyr.

3.2. *Coupling photocatalysis and adsorption units*

Fig. 7 shows the maximum selectivity values obtained after 8 minutes reaction with (red bars) and without (blue bars) adsorbent bed, by using bare and fluorinated TiO_2 at pH = 5.5 and 8.7, and by keeping constant the other experimental conditions (reaction volume 120 mL, flow rate 30 mL/min, initial Tyr concentration 0.5 mM). The striped portion of the red bars indicates the selectivity which would have been obtained without considering the Htyr desorbed from the adsorbent bed after the run, *i.e.* by only considering the Htyr detected in the recirculating solution. In the presence of the adsorbent bed, the selectivity towards Htyr almost doubled with respect to what obtained by considering only the reaction step for all of the considered cases. In particular, ca. 25 % selectivity could be obtained at pH = 8.7 in the presence of fluorinated TiO_2. This result is particularly relevant and represents a twofold increase in the selectivity towards Htyr with respect to the highest value ever reported in literature. It is worth mentioning that the values of selectivity calculated in the absence of the adsorbent bed (blue bars) are similar to those calculated without considering the amount of Htyr adsorbed onto the adsorbent bed (striped red bars). Notably, no significant variation on the amount of Tyr in the solution was observed in the presence of the adsorption unit, thus confirming the negligible adsorption of Tyr onto the bed.

The selectivity values have been calculated also for three separated runs lasting 8, 15 and 30 min, respectively, in the presence of fluorinated TiO_2 at pH = 8.7, under the experimental conditions described above. The values in the presence (red bars) and in the absence (blue bars) of the adsorbent bed are shown in Fig. 8.

It is evident that the selectivity trend in the presence of the adsorbent bed during time is similar to that reported in Fig. 6. Indeed, a maximum is observed at 8 min, while selectivity decreases for longer reaction times. For all the considered reaction times, the presence of the adsorption bed doubles the selectivity values.

To explain the remarkable effect of the adsorbent bed, it is necessary to describe more closely the chemical environment at its surface. The surface of the adsorbent exposes both boronic groups, grafted to the surface directly or through silane bridges, and free amino groups. These latter react through Lewis interactions with vicinal boronic groups, thus stabilizing tetracoordinated boronate moieties covalently linked to the support. In the absence of the amino groups, the boronate groups would exist only at pH > 8.7, i.e. above the pK_a of boronic acid. On the other hand, the presence of free amino groups at the surface of the adsorbent stabilizes the boronate moiety, which therefore can exist in water at much lower pH values. The existence of tetracoordinated boronate groups at circumneutral pH is of fundamental relevance for the aims of this investigation. In fact, as demonstrated in previous reports [25], only in this form boronate can selectively bind with molecules bearing catecholic functionalities, acting as a selective adsorption site for them, while showing negligible interaction with phenolic compounds. By inferring the same mechanism working also for Htyr and Tyr, showing the same functionalities, one can hypothesize that the Htyr photocatalytically produced could be selectively adsorbed at the surface of the adsorbent, while Tyr can be recycled back to the photocatalytic reacting unit. Fig. 9 schematically shows the stabilizing effect of amino groups on the boronate moieties, which therefore are capable of selectively binding Htyr molecules.

By considering that the presence of the adsorbent bed almost doubles the selectivity towards Htyr at both pH = 5.5 and 8.7, it can be concluded that its adsorbent efficiency is similar at both pH values. The higher selectivity obtained at pH = 8.7 can therefore be attributed

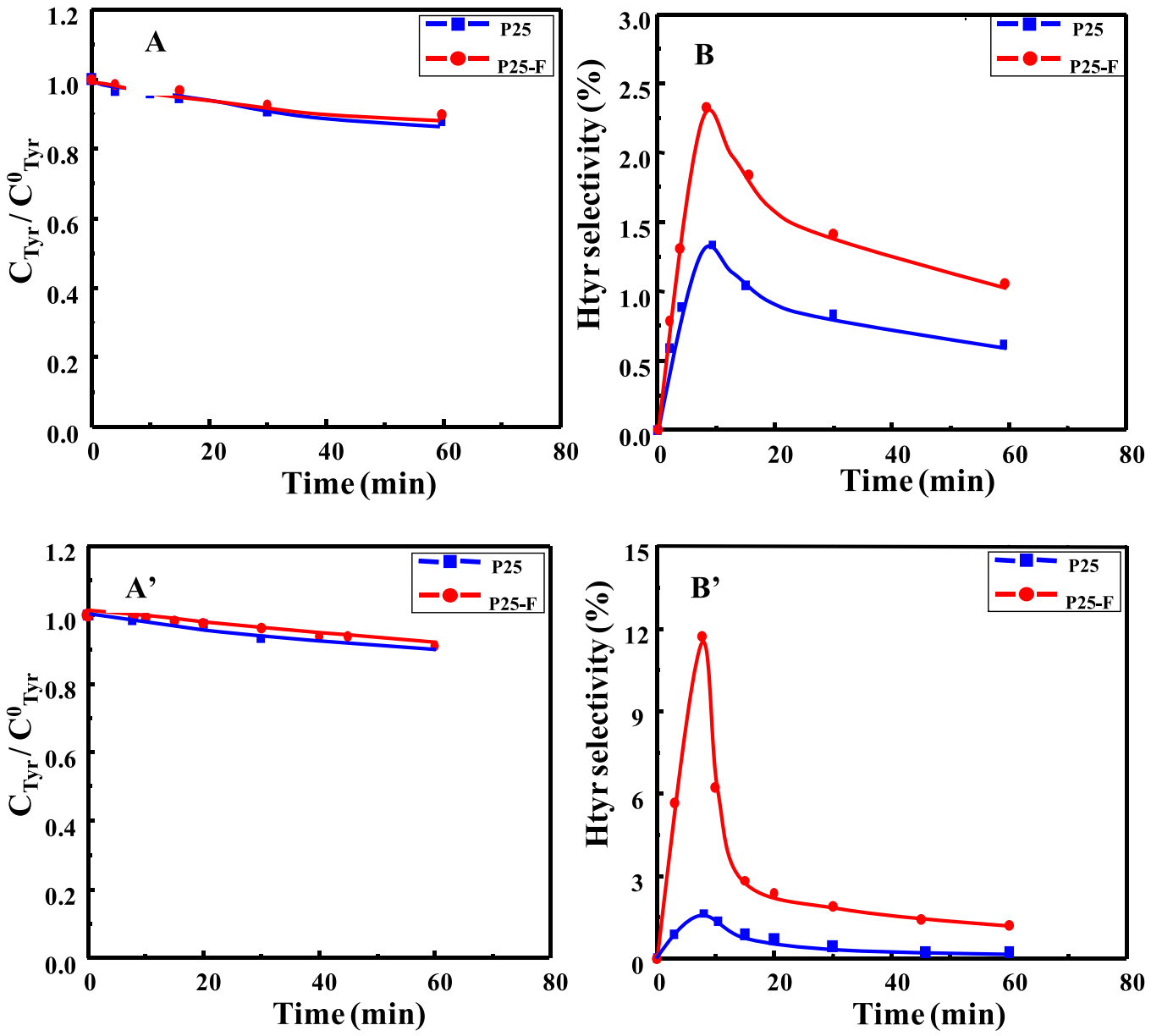

Fig. 6. Normalized concentration of Tyr and selectivity values towards Htyr at pH = 5.5 (A, B) and at pH = 8.7 (A', B'), in the presence of bare (blue squares) and fluorinated TiO_2 (red circles). Flow rate 30 mL/min, reaction volume 120 mL, initial Tyr concentration C^0_{Tyr} = 0.5 mM.

mainly to an improved efficiency of the reaction step at this pH (see Fig. 6) rather than to a beneficial effect of the adsorption bed. This finding highlights the remarkable effect of the amino groups stabilizing the boronate moieties even at circumneutral pH, extending the activity of the adsorbent out of the range of existence (pH $\geq$ 8.7) of isolated boronate groups [32].

3.3. Kinetic modeling and parameters estimation

The kinetic profiles of Tyr and Htyr during the photocatalytic experiments under various conditions were studied. Representative time-course data are presented in Fig. 10.

The kinetic data were analysed by hypothesizing the model depicted in the Scheme 1.

In this model, the transformation of Tyr to Htyr occurs via two parallel pathways. The first pathway is the direct hydroxylation, characterized by the kinetic constant k_1. The second pathway is a two-step process, characterized by the kinetic constants k_2 and k_3. The latter pathway involves the formation of the intermediate [I], which Bouguerra Neji et al., 2002 identified as the phenoxy radical [33], depicted in Fig. 11 by its three mesomeric forms [11].

The radical intermediate form [B] undergoes a rapid second electron transfer, followed by hydrolysis, resulting in the formation of Htyr (k_3). Htyr then participates in additional reactions (k_4) that produce secondary products (referred to as P_1) and is subsequently removed from the reaction medium. In the presence of an adsorbent bed, this process may also involve adsorption onto the substrate, further eliminating Htyr from the reaction medium. Similarly, the radical [C] proceeds through a series of reactions (k_5) that ultimately lead to the formation of hydroxyquinone and other secondary products (referred to as P_2).

The rate of formation/disappearence of each species that is involved in the five-step model can be represented by the following set of ordinary differential equations (Eqs. 1–5):

$$\frac{d[Tyr]}{dt} = -k_1[Tyr] - k_2[Tyr] + k_{-2}[I] \quad (1)$$

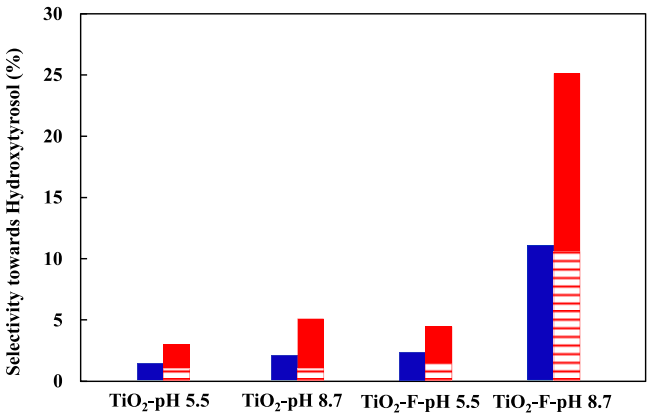

Fig. 7. Maximum selectivity values towards Htyr obtained after 8 minutes with (red bars) and without (blue bars) adsorbent bed, by using bare and fluorinated TiO_2 at pH = 5.5 and 8.7, and by keeping constant the other experimental conditions (reaction volume 120 mL, flow rate 30 mL/min, initial Tyr concentration 0.5 mM).

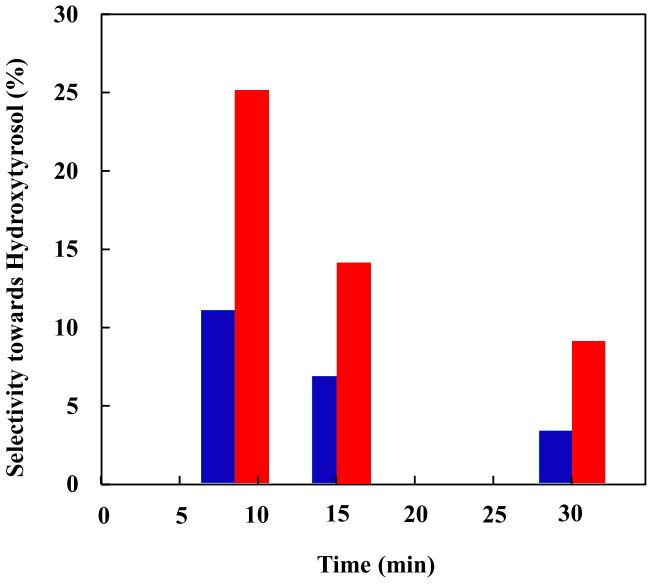

Fig. 8. Selectivity values towards Htyr obtained in the presence (red bars) and in the absence (blue bars) of the adsorbent bed obtained in separated runs lasting 8, 15 and 30 minutes. Reaction volume 120 mL, flow rate 30 mL/min, initial Tyr concentration C^0_{Tyr} = 0.5 mM, pH = 8.7.

$$\frac{d[Htyr]}{dt} = k_1[Tyr] + k_3[I] - k_4[Htyr] \quad (2)$$

$$\frac{d[I]}{dt} = k_2[Tyr] - k_3[I] - k_5[I] \quad (3)$$

$$\frac{d[P_1]}{dt} = k_4[Htyr] \quad (4)$$

$$\frac{d[P_2]}{dt} = k_5[I] \quad (5)$$

The apparent rate parameters (Table 1) for each set of experimental conditions were estimated by simultaneously solving the rate laws reported above. This was achieved by minimizing the objective function using the Evolutionary Programming feature of COPASI 4.39.

It has been observed that while the flow rate does not influence the values of the kinetic constants (the values reported in the table are

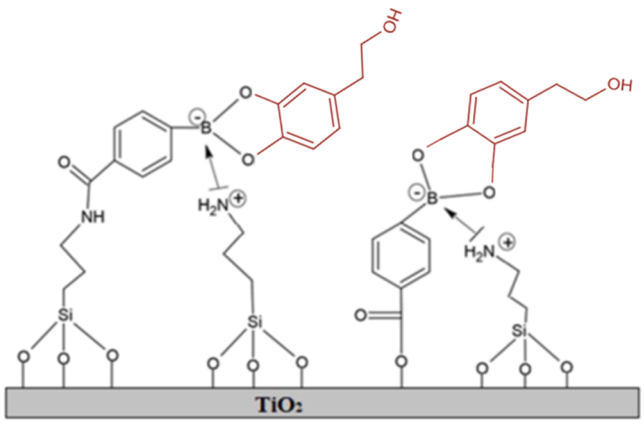

Fig. 9. Scheme of the interaction between Htyr and amine stabilized boronate moieties at the surface of the adsorbent.

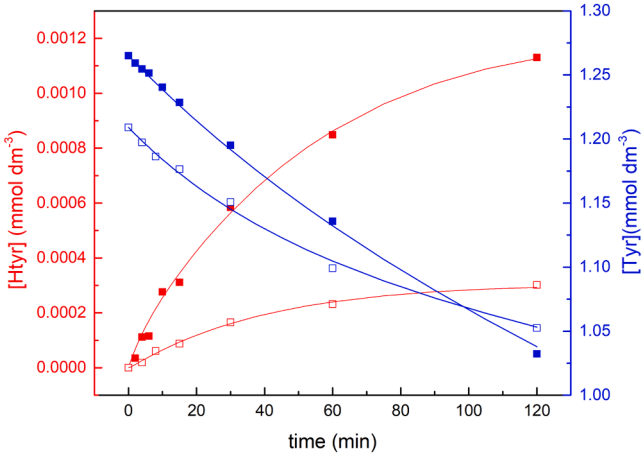

Fig. 10. Typical kinetic profiles for Tyr (■) and Htyr (■) in the absence (A) and presence (B) of the adsorbent bed. Reaction volume 120 mL, pH = 8.7, flow rate 30 mL/min. The lines represent simulations obtained using the model described in Scheme 1.

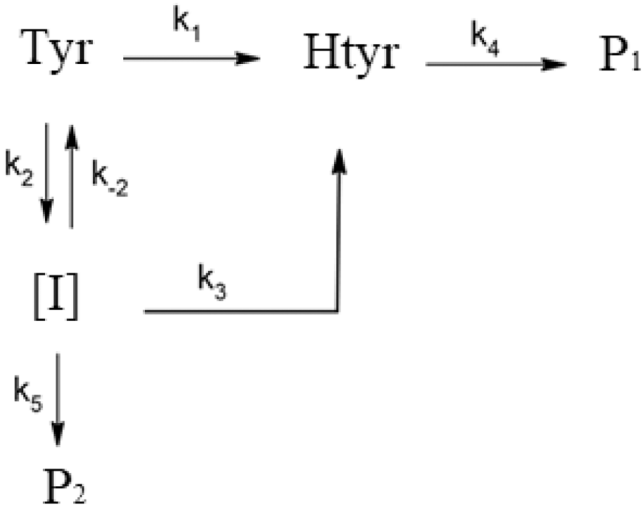

Scheme 1. Reaction pathway of Tyr oxidation.

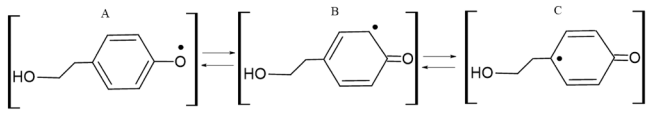

Fig. 11. Chemical structure of the the mesomeric forms of the intermediate I.

Table 1
Rate constant values obtained from the simultaneous fitting of the kinetic profiles of Tyr and Htyr during photocatalytic runs, both in the absence and presence of the adsorbent bed. The reported values are the averages of those obtained under various experimental conditions (flow rate, reactor volume, and initial Tyr concentration).

	Without adsorbent bed	With adsorbent bed
k_1 (min^{-1})	$(4.1 \pm 0.2) \cdot 10^{-5}$	$(2.2 \pm 0.5) \cdot 10^{-5}$
k_2 (min^{-1})	$(2.38 \pm 0.07) \cdot 10^{-3}$	$(2.45 \pm 0.06) \cdot 10^{-3}$
k_{-2} (min^{-1})	$(5.3 \pm 0.9) \cdot 10^{-3}$	$(6 \pm 1) \cdot 10^{-3}$
k_3 (min^{-1})	$(7 \pm 1) \cdot 10^{-4}$	$(3.70 \pm 0.09) \cdot 10^{-3}$
k_4 (min^{-1})	0.21 ± 0.05	1.45 ± 0.03
k_5 (min^{-1})	$(1.3 \pm 0.2) \cdot 10^{-3}$	$(1.5 \pm 1) \cdot 10^{-8}$

averages), the presence of the adsorbent significantly affects the rate of certain processes. Specifically, there is a marked increase in the disappearance rate of Htyr (k_4). This increase can reasonably be attributed to the adsorption process, as Htyr exhibits a high affinity for the adsorbent used.

Furthermore, the presence of the adsorbent leads to a marked decrease in the disappearance rate of the intermediate radical (k_5) and an increase in its transformation rate into Htyr (k_3). These changes suggest that the adsorption of Htyr onto the support effectively removes this product from the reaction medium, thereby promoting its greater production.

Lastly, a slight decrease is observed in the direct oxidation rate of Tyr (k_1), which is likely a result of the increased rate of Htyr formation through intermediate formation.

The proposed mechanism and the observed changes in kinetic constants underscore the efficacy of the adsorbent in selectively enhancing the production of Htyr.

4. Conclusions

In this work, a photocatalytic totally recycled flow reactor performing the partial oxidation of tyrosol (Tyr) to hydroxytyrosol (Htyr) was coupled with a selective adsorption unit. Preliminary photocatalytic runs, performed in the absence of the adsorption unit, showed that the reaction provided a maximum selectivity of 12 % in the presence of fluorinated TiO_2 at pH = 8.7. Reducing the residence time from 4 to 0.89 min did not result in selectivity enhancement. Performing this partial oxidation in opportunely designed microreactors could possibly further reduce the residence time, thus providing beneficial effects in terms of reaction performances. On the other hand, in the presence of the adsorption unit, the selectivity towards Htyr could be doubled up to 25 %. The adsorbent, in fact, exposing at the surface boronate moieties stabilized by vicinal amino groups, was able to selectively remove the target product (Htyr) from the reacting medium, while leaving almost unaltered the concentration of the reactant (Tyr). The kinetic of the reaction has been modelled by considering both the reaction and the adsorption units, and the relevant constants governing the process have been retrieved.

CRediT authorship contribution statement

Leonardo Palmisano: Writing – review & editing, Supervision. **Francesco Parrino:** Writing – review & editing, Writing – original draft, Validation, Supervision, Project administration, Methodology, Formal analysis, Data curation, Conceptualization. **Hiba Khlifi:** Writing – original draft, Visualization, Investigation, Formal analysis, Data curation. **Filippo Parisi:** Writing – review & editing, Visualization, Validation, Methodology, Investigation, Data curation, Conceptualization. **Luciana Sciascia:** Writing – review & editing, Visualization, Validation, Methodology, Formal analysis, Data curation, Conceptualization.

Declaration of Competing Interest

The authors declare that they have no known competing financial interests or personal relationships that could have appeared to influence the work reported in this paper.

Data Availability

Data will be made available on request.

Appendix A. Supporting information

Supplementary data associated with this article can be found in the online version at doi:10.1016/j.cattod.2024.115053.

References

[1] C. Romero, M. Brenes, Analysis of total contents of hydroxytyrosol and tyrosol in olive oils, J. Agric. Food Chem. 60 (2012) 9017–9022.
[2] M. Bertelli, A.K. Kiani, S. Paolacci, E. Manara, D. Kurti, K. Dhuli, V. Bushati, J. Miertus, D. Pangallo, M. Baglivo, T. Beccari, S. Michelini, Hydroxytyrosol: a natural compound with promising pharmacological activities, J. Biotechnol. 309 (2020) 29–33.
[3] FACT3533MR, Market research survey-Hydroxytyrosol Market, 2022.
[4] C.S. Papageorgiou, P. Lyri, I. Xintaropoulou, I. Diamantopoulos, D.A.-O. Zagklis, C. A.-O. Paraskeva, High-yield production of a rich-in-hydroxytyrosol extract from olive (Olea europaea) Leaves, Antioxidants 11 (2022) 1042.
[5] D.F. Tirado, E. Fuente, L. Calvo, A selective extraction of hydroxytyrosol rich olive oil from alperujo, J. Food Eng. 263 (2019) 409–416.
[6] K. Napora-Wijata, K. Robins, A. Osorio-Lozada, M. Winkler, Whole-cell carboxylate reduction for the synthesis of 3-hydroxytyrosol, ChemCatChem 6 (2014) 1089–1095.
[7] A.D. Kalampaliki, V. Giannouli, A.L. Skaltsounis, I.K. Kostakis, A three-step, gram-scale synthesis of hydroxytyrosol, hydroxytyrosol acetate, and 3,4-dihydroxyphenylglycol, Molecules 24 (2019) 3239.
[8] E.M. Roberta Bernini, Maurizio Barontini, Fernanda Crisante, Method for preparing hydroxytyrosol derivatives and of hydroxytyrosol, Patent n° WO2008110908A1, (2008).
[9] J. Britton, R. Davis, K.E. O'Connor, Chemical, physical and biotechnological approaches to the production of the potent antioxidant hydroxytyrosol, Appl. Microbiol. Biotechnol. 103 (2019) 5957–5974.
[10] F.A.-O. Annunziata, M.L. Contente, C.A.-O. Pinna, L.A.-O. Tamborini, A.A.-O. Pinto, Biocatalyzed flow oxidation of tyrosol to hydroxytyrosol and efficient production of their acetate esters, Antioxidants 10 (2021) 1142.
[11] S. Bouguerra Neji, M. Bouaziz, Production of biologically active hydroxytyrosol rich extract via catalytic conversion of tyrosol, RSC Adv. 12 (2022) 2595–2602.
[12] F. Parrino, L. Palmisano, Reactions in the presence of irradiated semiconductors: Are they simply photocatalytic? Mini-Rev. Org. Chem. 15 (2018) 157–164.
[13] F. Parrino, G. Camera Roda, V. Loddo, L. Palmisano, Green synthesis of bromine by TiO_2 heterogeneous photocatalysis and/or ozone: a kinetic study, J. Catal. 366 (2018) 167–175.
[14] F. Parrino, S. Livraghi, E. Giamello, L. Palmisano, The existence of nitrate radicals in irradiated TiO_2 aqueous suspensions in the presence of nitrate ions, Angew. Chem. Int. Ed. 57 (2018) 10702–10706.
[15] F. Parrino, C. DePasquale, L. Palmisano, Influence of surface-related phenomena on mechanism, selectivity, and conversion of TiO_2-induced photocatalytic reactions, ChemSusChem 12 (2019) 589–602.
[16] H. Khlifi, F. Parisi, L. Elsellami, G. Camera-Roda, L. Palmisano, R. Ceccato, F. Parrino, Photocatalytic partial oxidation of tyrosol: improving the selectivity towards hydroxytyrosol by surface fluorination of TiO_2, Top. Catal. 63 (2020) 1350–1360.
[17] R. Binjhade, R. Mondal, S. Mondal, Continuous photocatalytic reactor: critical review on the design and performance, J. Environ. Chem. Eng. 10 (2022) 107746.
[18] I. Rossetti, M. Compagnoni, Chemical reaction engineering, process design and scale-up issues at the frontier of synthesis: flow chemistry, Chem. Eng. J. 296 (2016) 56–70.
[19] M.J. Lima, A.M.T. Silva, C.G. Silva, J.L. Faria, N.M. Reis, Selective photocatalytic synthesis of benzaldehyde in microcapillaries with immobilized carbon nitride, Chem. Eng. J. 430 (2022) 132643.
[20] C.A.-O. Thomson, A.A.-O. Lee, F.A.-O. Vilela, Heterogeneous photocatalysis in flow chemical reactors, Beilstein J. Org. Chem. 16 (2020) 1495–1549.

[21] G. Camera-Roda, V. Loddo, L. Palmisano, F. Parrino, F. Santarelli, Process intensification in a photocatalytic membrane reactor: analysis of the techniques to integrate reaction and separation, Chem. Eng. J. 310 (2017) 352–359.
[22] G. Camera-Roda, A. Cardillo, V. Loddo, L. Palmisano, F. Parrino, Improvement of membrane performances to enhance the yield of vanillin in a pervaporation reactor, Membranes 4 (2014) 96–112.
[23] G. Camera-Roda, F. Parrino, V. Loddo, L. Palmisano, A. Dialysis, photocatalytic reactor for the green production of vanillin, Catalysts 10 (2020) 326.
[24] G. Camera-Roda, V. Loddo, L. Palmisano, F. Parrino, Green synthesis of vanillin: pervaporation and dialysis for process intensification in a membrane reactor, Chem. Eng. Trans. 75 (2019) 1–6.
[25] H. Khlifi, E. Callone, F. Parisi, L. Sciascia, L. Palmisano, S. Dirè, F. Parrino, Amine-stabilized boronate groups at the surface of modified TiO_2 under circumneutral pH conditions: application to selective photocatalytic degradations, J. Photochem. Photobiol. A: Chem. 444 (2023) 114903.
[26] F. Parisi, L. Sciascia, H. Khlifi, L. Elsellami, D. Lenaz, F. Princivalle, F. Parrino, Interaction of phenolic compounds with functionalized TiO_2: enhanced catechol adsorption and cooperative phenol adsorption, Ceram. Int. (2024).
[27] S. Hoops, S. Sahle, R. Gauges, C. Lee, J. Pahle, N. Simus, M. Singhal, L. Xu, P. Mendes, U. Kummer, COPASI—a COmplex PAthway SImulator, Bioinformatics 22 (2006) 3067–3074.
[28] G. Camera-Roda, V. Loddo, L. Palmisano, F. Parrino, Photocatalytic ozonation for a sustainable aquaculture: a long-term test in a seawater aquarium, Appl. Catal. B: Environ. 253 (2019) 69–76.
[29] N. Fessi, M. Faouzi Nsib, L. Cardenas, C. Guillard, F. Dappozze, A. Houas, F. Parrino, L. Palmisano, G. Ledoux, D. Amans, Y. Chevalier, Surface and electronic features of fluorinated TiO_2 and their influence on the photocatalytic degradation of 1-methylnaphthalene, J. Phys. Chem.: C. (2020).
[30] N. Fessi, M.F. Nsib, Y. Chevalier, C. Guillard, F. Dappozze, A. Houas, L. Palmisano, F. Parrino, Pickering emulsions of fluorinated TiO_2: a new route for intensification of photocatalytic degradation of nitrobenzene, Langmuir 36 (2020) 13545–13554.
[31] N. Schweigert, R.I. Zehnder Aj Fau - Eggen, R.I. Eggen, Chemical properties of catechols and their molecular modes of toxic action in cells, from microorganisms to mammals, Environmental Microbiology 3 (2001) 81–91.
[32] J.P. Lorand, J.O. Edwards, Polyol complexes and structure of the benzeneboronate ion, J. Org. Chem. 24 (1959) 769–774.
[33] S. Bouguerra Neji, M. Bouaziz, Production of biologically active hydroxytyrosol rich extract via catalytic conversion of tyrosol, RSC Adv. 12 (2022) 2595–2602.